Engineering optical anisotropy in nonlinear crystals with ultrafast light

Cite as: J. Appl. Phys. **127**, 153104 (2020); https://doi.org/10.1063/5.0003589
Submitted: 03 February 2020 • Accepted: 02 April 2020 • Published Online: 20 April 2020

Pawel Karpinski, Vladlen Shvedov, Wieslaw Krolikowski, et al.

Journal of Applied Physics ARTICLE scitation.org/journal/jap

Engineering optical anisotropy in nonlinear crystals with ultrafast light

Cite as: J. Appl. Phys. **127**, 153104 (2020); doi: 10.1063/5.0003589
Submitted: 3 February 2020 · Accepted: 2 April 2020 ·
Published Online: 20 April 2020

Pawel Karpinski,[1,2,a)] Vladlen Shvedov,[1] Wieslaw Krolikowski,[1,3] and Cyril Hnatovsky[4]

AFFILIATIONS

[1]Research School of Physics, Australian National University, Canberra, ACT 2600, Australia
[2]Wroclaw University of Science and Technology, 50-370 Wroclaw, Poland
[3]Texas A&M University at Qatar, 00000 Doha, Qatar
[4]Security and Disruptive Technologies Research Centre, National Research Council of Canada, Ottawa, Ontario K1A 0R6, Canada

[a)]**Author to whom correspondence should be addressed:** pawel.karpinski@pwr.edu.pl

ABSTRACT

Photonic technology is widely based on anisotropic (and) nonlinear materials, which allow light modulation and parametric light conversion. Because the number of naturally occurring crystals is limited, there is a growing demand for artificial metamaterials with optical properties specifically tailored to a given application. Here, we utilize the top-down method to synthesize sub-wavelength periodic nanostructures inside a uniaxial optically nonlinear crystal (lithium niobate, $LiNbO_3$) by irradiating it with multiple femtosecond laser pulses. By superimposing form-birefringence associated with the light-induced nanostructures onto natural birefringence of the host crystal we create macroscopic domains of a biaxial metamaterial embedded into otherwise uniaxial medium.

Laser irradiation of a transparent (at the laser wavelength) solid with focused femtosecond laser pulses provides a unique opportunity to remotely modify its properties. Three-dimensional (3D) modification of transparent bulk materials—first shown in 1996 in the context of data storage[1] and waveguide fabrication[2] in glass—is now a mature technology widely used both in the laboratory and industrial environment.[3–10] The way in which a transparent material is modified critically depends on a selected combination of several laser-writing parameters, such as the pulse energy (E), pulse duration (τ),[11] numerical aperture of the pulse focusing optics (NA),[12] laser polarization,[7,13,14] number of laser pulses deposited per unit volume (N),[7,13,14] and pulse repetition rate (f).[15,16] Nevertheless, modification of any transparent material requires the focused light intensity to be above the nonlinear photoionization threshold,[17,18] which immediately imposes strict limitations on the choice of E, τ, and NA. For fixed τ and NA, material modification inside the laser-irradiated region typically proceeds through three distinct phases as the pulse energy E is increased: a weak homogeneous increase (or decrease) of the refractive index, the index change saturation and, finally, material damage/disruption. Interestingly, for some glasses[19–25] and crystals (including lithium niobate, $LiNbO_3$),[10,26–28] there exists a range of parameters, below the material damage threshold, when the light–matter interaction inside the material volume leads to the formation of sub-wavelength self-organized periodic structures (i.e., nanogratings) oriented perpendicularly to the electric vector of the laser pulses. This controlled material modification has been extensively used over the past decade to either change the material properties of a transparent medium in order to selectively increase its etching rate[7,8] or engineer the refractive index of a transparent medium via inducing form-birefringence in it.[29–32] In the case of $LiNbO_3$, the modified material exhibits two kinds of birefringence: natural birefringence and form-birefringence originating from the presence of light-induced nanogratings. Importantly, the ability to control the orientation of nanogratings with the pulse polarization allows one to vary the spatial orientation and strength of the induced form-birefringence. In view of the recent advances in 3D femtosecond laser modification of linear and nonlinear crystals,[33–38] $LiNbO_3$ with tailored optical properties and incorporated microphotonic components becomes a reality. The very possibility of making such a unique device opens up unprecedented opportunities in the design of optical circuits for signal guiding and processing, frequency conversion, and beam shaping.

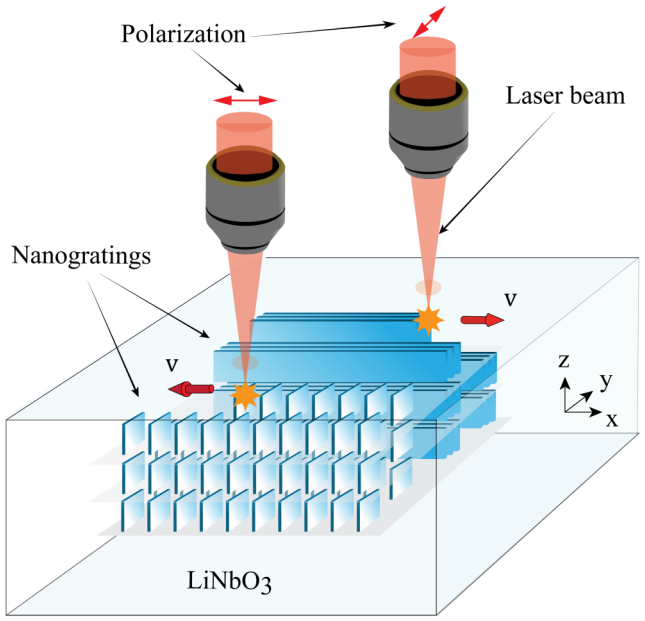

FIG. 1. Schematic illustration of the formation of light-induced self-organized nanogratings inside $LiNbO_3$. **v** denotes the laser writing speed.

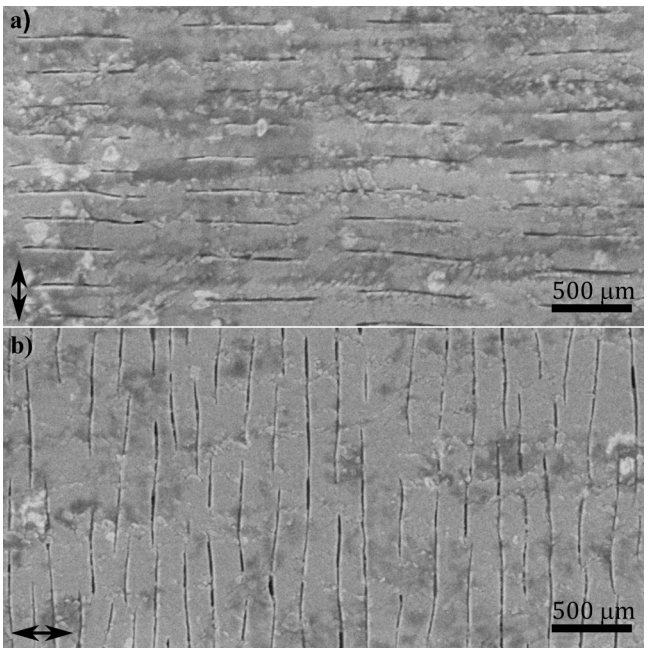

FIG. 2. SEM images (a) of the nanogratings formed inside MgO:$LiNbO_3$ crystal, as revealed by etching the sample for 20 s in a 49% solution of hydrofluoric acid (HF). The pulse energy is $E = 0.5\,\mu$J; the separation between the lines scanned by the laser beam is equal to $1\,\mu$m. The writing direction is vertical and the polarization of the writing light polarization is (a) vertical and (b) horizontal.

A schematic of the femtosecond laser writing setup is shown in Fig. 1. A $370\,\mu$m thick sample of monocrystalline Z-cut 5 mol. % magnesium-oxide-doped lithium niobate (MgO:$LiNbO_3$) was irradiated with laser pulses from a regenerative amplifier ($\tau = 200$ fs, $f = 100$ kHz, central wavelength $\lambda = 800$ nm). The linearly polarized laser beam was focused inside the sample $70–300\,\mu$m below the surface using a NA = 0.65 microscope objective allowing depth-dependent compensation of spherical aberration induced by the air–$LiNbO_3$ planar interface.[39,40] The focal spot diameter D inside the sample was estimated at $D = \frac{2\lambda}{\pi \mathrm{NA}} = 0.8\,\mu$m. The sample was translated in the XY-plane along either the X axis or Y axis at a speed $v = 100\,\mu$m/s, leading to irradiation of the material with approximately $N = 1000$ light pulses per spot. The light–matter interaction in the sample resulted in material modification in the form of self-organized nanogratings. We note that the selected laser-writing conditions were conducive to nanograting formation as they ensured that the focused intensity exceeded levels necessary for weak material modification, such as light-induced stress and photorefractive effect,[7] but was lower than the damage threshold.

To reveal the laser-induced nanostructures inside the material, our sample was first polished from the top in order to remove the unmodified layer and then etched in a 49% solution of hydrofluoric acid (HF) for 20 s. The top view SEM images of the laser-induced nanostructures are depicted in Fig. 2. These particular structures were formed by scanning the crystal along vertical (Y axis) lines with a $1\,\mu$m separation along the X axis between subsequent lines. The polarization of the writing beam was set as vertical [Fig. 2(a)]) or horizontal [Fig. 2(b)]). It can be seen that, in accordance with earlier results,[26] the orientation of nanogratings is always perpendicular to the polarization of the writing light. Interestingly, we did not observe any influence of the crystalline structure on the gratings formation, hence nanogratings could be written along any direction in the XY-plane of the $LiNbO_3$ crystal. Similarly, the same nanostructures were obtained for the laser beam incident from either –Z- or +Z-surface of the sample. Based on the SEM images, the average period of the nanogratings was measured to be $\Lambda \approx 210$ nm. As can be seen from Fig. 2(a), the material modification was produced with a sub-diffraction resolution as the width of modified material was only 0.5 m, i.e., significantly smaller than the focal spot diameter D estimated at 0.8 m. This is an effect of a multi-photon process, and, with correct adjustment of the pulse energy E and writing speed v, it is possible to produce modification consisting of only one or two lines (cracks).[27]

The presence of nanogratings inside $LiNbO_3$ introduces strong form birefringence to the crystal. This effect, which is caused by a sub-wavelength variation of the refractive index of the material, has been demonstrated before inside fused silica (SiO_2).[19,20,41] In that case, it transformed the otherwise optically isotropic material into a birefringent medium, i.e., a uniaxial metamaterial.

Figure 3 shows polarization microscopy images of the fabricated structures. Each $50 \times 50\,\mu$m^2 square structure was made of 100 lines written at $v = 100\,\mu$m/s and separated by a $0.5\,\mu$m distance. This ensured uniform coverage of the modified volume with

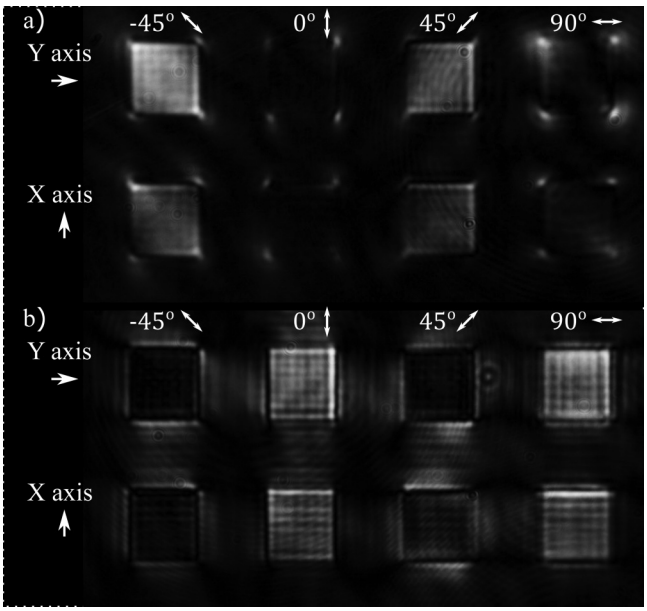

FIG. 3. Cross-polarized images of light-induced self-organized nanogratings inside MgO:$LiNbO_3$, with the polarizer and analyser oriented at (a) 0° and 90°, respectively, and (b) 45° and −45°, respectively. The structures are written along the X axis or Y axis (white arrows on the left side of the Fig. 3), with the light polarization oriented at −45°, 0°, 45°, and 90° (white arrows at the top).

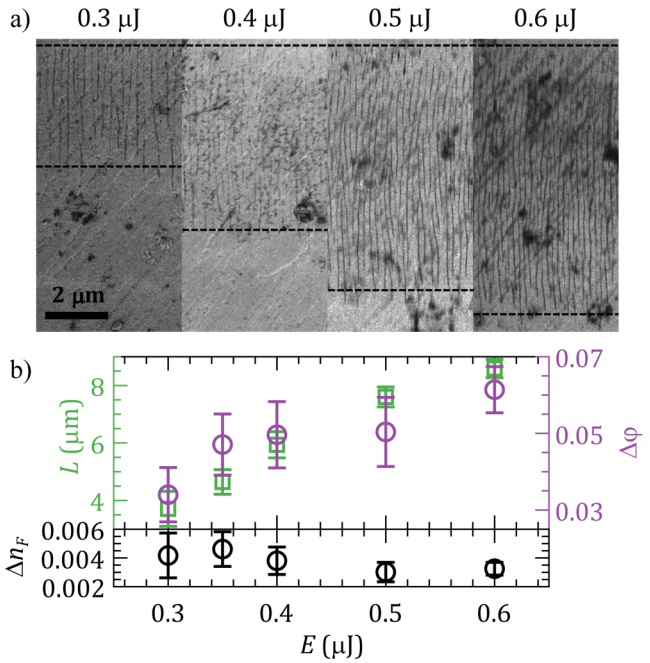

FIG. 4. (a) Cross-sectional (XZ-plane) SEM images of the nanogratings in $LiNbO_3$ written with different pulse energies E. (b) Top: extent L of the modified material (i.e., nanogratings) estimated from the SEM images in Fig. 4(a), and phase shift $\Delta\varphi$ induced by the nanogratings, measured at 455 nm, as a function of E. Bottom: form birefringence Δn_F calculated from $\Delta\varphi$ and L.

nanogratings. Additionally, all sample were annealed on a hot plate for an hour at 250 °C, after laser writing, to remove any photorefractive effect, which could compete with form birefringence. The orientation of the nanogratings within the irradiated regions was varied by rotating the linear polarization of the writing laser beam, as shown in Fig. 3. The images of the sample placed between two crossed polarizers represent situations when the polarizer and analyser were aligned along 0° and 90°, respectively [Fig. 3(a)], and along −45° and 45°, respectively [Fig. 3(b)]. It can be seen that the direction of the induced optical axis is always perpendicular to the polarization direction of the writing laser beam. Also notice the presence of weak stress-induced birefringence, which is localized in the corners of the fabricated structures and regions proximate to the fabricated structures.

In order to measure form birefringence induced by subwavelength nanostructures, we produced a number of structures using pulse energies in the range $E = 0.3 - 0.6\mu J$. To minimize aberrations and avoid focus-splitting effects, we focused the beam close to the front surface of the wafer.[26,42–44] The phase shift $\Delta\varphi$ between the ordinary and extraordinary polarization components of light passing through the produced structures was measured using a Soleil-Babinet compensator. The extent L of the structures along the beam propagation direction (Z axis) was deduced from the SEM images shown in Fig. 4(a). For that purpose, the sample was cut along the plane perpendicular to the formed nanogratings (XZ-plane), polished and then etched in HF to accentuate the modification morphology. Figure 4(b) shows how L increases with the pulse energy E, whereas the top panel of Fig. 4(b) presents $\Delta\varphi$ as a function of E. Clearly, both L and $\Delta\varphi$ grow with E in a similar fashion. As a result, the form birefringence Δn_F (i.e., the difference between the ordinary and extraordinary refractive index of the nanograting) is almost independent of the pulse energy in the range $E = 0.3 - 0.6\mu J$ and is equal to $\Delta n_F = 0.0038$, as measured at a 455 nm wavelength [the bottom panel of Fig. 4(b)].

Knowing the value of form birefringence, one can estimate the width w of thin layers of laser-modified material inside nanogratings. Assuming that (1) the layer width w is much smaller than the nanograting period Λ (i.e., $w \ll \Lambda$), (2) the refractive index of the material between the layers (for $LiNbO_3$, $n_o = 2.3743$, $n_e = 2.2770$ at a wavelength of 455 nm[45]) is not affected by the laser exposure, and (3) the refractive index profile across the layers is described by a step-like function, the form birefringence can be approximated by[7,31]

$$\Delta n_F = \frac{2}{\Lambda}\left(\frac{\delta n^2}{n_o} + \frac{\delta n^3}{n_o^2}\right)w, \tag{1}$$

where $\delta n = n_o - n_m$ and n_m is the refractive index of the layers. In the limiting case when $n_m = 1$, which corresponds to a nanocrack,[7,11] Eq. (1) gives a nanocrack width of $w \approx 3$ Å. This would mean that such nanocracks are disruptions in the material that are smaller than the lattice constant of the $LiNbO_3$ crystal

($a = 5.148$ Å in the xy crystallographic plane),[46] which is unlikely because the modified material seems to be impermeable to liquids (isopropanol).[47] Based on this, we are not dealing with real physical voids (empty space), but rather with a more complex type of material modification, e.g., amorphous material. The amorphous material would then be etched much faster than the host crystalline material, making the layers visible on the SEM images. Assuming that the refractive index inside the modified layers is $n_m = 2.14$, i.e. that of amorphous $LiNbO_3$,[48] we find the width of the changed material to be $w \approx 15.7$ nm, which corresponds to the value estimated from the SEM images shown in Fig. 2.

Combining light-induced form birefringence with natural birefringence of the uniaxial $LiNbO_3$ crystal gives rise to artificial optical biaxiality of the crystal. The natural birefringence $\Delta n_{nat} = -0.0973$ (at 455 nm wavelength) is more than an order of magnitude larger than the induced form birefringence. Even though the nanogratings are confined to the XY crystallographic plane, they affect the refractive index in all crystallographic directions including the Z-direction. Using the effective medium theory (EMT),[29,30,49] we can calculate changes in the refractive index induced by nanograting structures in each direction (X, Y, and Z).

The matrix of natural refractive indices can be written as

$$\hat{n}^2 = \begin{bmatrix} n_{11}^2 & 0 & 0 \\ 0 & n_{22}^2 & 0 \\ 0 & 0 & n_{33}^2 \end{bmatrix} = \begin{bmatrix} n_o^2 & 0 & 0 \\ 0 & n_o^2 & 0 \\ 0 & 0 & n_e^2 \end{bmatrix}, \tag{2}$$

where n_o and n_e are the ordinary index and extraordinary refractive index, respectively. Nanogratings induced in the direction perpendicular to the X axis lead to a new refractive index:

$$\widehat{n_F}^2 = \begin{bmatrix} {n_{F,11}}^2 & 0 & 0 \\ 0 & {n_{F,22}}^2 & 0 \\ 0 & 0 & {n_{F,33}}^2 \end{bmatrix} = \begin{bmatrix} \dfrac{{n_{11}}^2 {n_m}^2 \Lambda}{w\,{n_{11}}^2 + (\Lambda - w){n_m}^2} & 0 & 0 \\ 0 & \dfrac{(\Lambda - w)\,{n_{22}}^2 + w\,{n_m}^2}{\Lambda} & 0 \\ 0 & 0 & \dfrac{(\Lambda - w)\,{n_{33}}^2 + w\,{n_m}^2}{\Lambda} \end{bmatrix}. \tag{3}$$

Substituting the values of $n_o = 2.3743$, $n_e = 2.2770$, $n_m = 2.14$, $w = 15.7$ nm and $\Lambda = 210$ nm for $LiNbO_3$ into Eq. (3), we obtain the refractive indices of the new biaxial metamaterial,

$$\widehat{n_F} = \begin{bmatrix} 2.354 & 0 & 0 \\ 0 & 2.358 & 0 \\ 0 & 0 & 2.267 \end{bmatrix}.$$

From this we can calculate the acute angle $2V_z$ between the optical axes of this artificial biaxial medium as[30,31,50]

$$2V_z = 2\cos^{-1}\left(\frac{n_{F,22}}{n_{F,11}}\sqrt{\frac{n_{F,11}^2 - n_{F,33}^2}{n_{F,22}^2 - n_{F,33}^2}}\right). \tag{4}$$

After substituting the values of the refractive indices of the artificial biaxial material into Eq. (4), we obtain $2V_z = 22.12°$ (0.386 rad) at 455 nm.

We employed conoscopic microscopy to experimentally study anisotropy of the modified material. To this end, we first uniformly covered a macroscopic volume of a Z-cut, 370 μm-thick $LiNbO_3$ crystal with nanogratings. The fabricated structure extended over a $100 \times 100\,\mu m^2$ area in the XY-plane and was 250 μm-thick along the Z-direction. In order to minimize the stress induced by the laser writing process and, consequently, to avoid potential cracking at the boundaries of the laser-modified region, the structure was of a cylindrical shape, with a base diameter of 100 μm. The lines of material modification were written with a 0.5 μm separation in the XY-plane and a 5 μm separation along the Z-direction. The structure was fabricated with the same laser polarization layer-by-layer (in the XY-plane) starting from the bottom and moving up in the negative Z-direction, with the laser writing direction in each layer being oriented at a right angle with respect to the previous layer (i.e., first along X, then along Y, then, again, along X, etc.). As the structure was thick and positioned deep inside the medium, we had to adjust compensation for interface-induced spherical aberration every 50 μm along Z. In the end, the cylindrical region containing nanogratings was sandwiched between a 70 μm layer of the pristine $LiNbO_3$ wafer at the top and a 50 μm layer at the bottom.

Figure 5(a) shows an optical image of the produced macroscopic structure. It can be seen that the structure in not fully transparent. The optical losses were deduced from transmission spectra of a halogen lamp, recorded through unmodified $LiNbO_3$ and through the produced structure. The optical losses [Fig. 5(b)] decrease with increasing the probe light wavelength as λ^{-3}. This indicates that the scattering in the structure occurs both on inhomogeneities that are much smaller or comparable to the probe light wavelength, i.e., it is a combination of Rayleigh and Mie scattering, in which Rayleigh scattering dominates.[51,52] The measured optical losses are 3 dB/mm at 800 nm, which is acceptable for integrated optical circuits.

Our conoscopic microscope was based on the classical configuration that incorporates a condenser lens and an objective lens to illuminate and view the sample from different angles in a cone of light. In our case, we used two microscope objectives of NA = 0.65

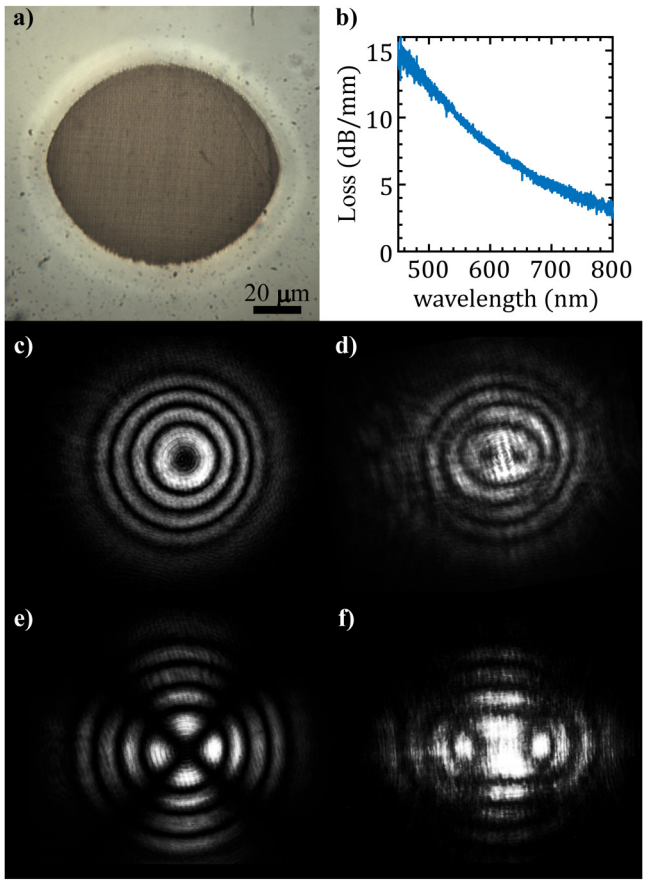

FIG. 5. (a) An optical microscopy image of the macroscopic laser-written structure (i.e., artificial biaxial metamaterial) described in the text. (b) Wavelength-dependent optical losses in the structure. (c), (d), (e) and (f) Averaged conoscopic images of the structure. (c) and (d) Conoscopic images with circularly polarized light; (e) and (f) conoscopic images with linearly cross-polarized light (incident polarization is at 45°); (c) and (e) 370 μm-thick pristine $LiNbO_3$ crystal, (d) and (f) 250 μm-thick biaxial metamaterial embedded into the pristine $LiNbO_3$ crystal.

each as the condenser and the imaging objective.[53–55] The intensity and polarization of the incoming He–Ne laser light (~633 nm) were maintained using half-wave and quarter-wave plates and a polarizer. We performed observation for circular and linear polarization, with an appropriate analyser system placed in front of a CCD camera. Since the fabricated nanogratings are not ideally uniform and scatter light, and we used a coherent light source, we had to perform averaging of data to minimize the effect of noise. To this end, we set a long exposure time on the CCD camera and translated the sample in random directions at random speed. For consistency, we applied the same procedure for the observation of the reference pristine $LiNbO_3$ crystal.

The conoscopic images shown in Figs. 5(c)–5(f) are all composed of concentric isochromates. Figures 5(e) and 5(f) also show isogyres, which form the characteristic cross in Fig. 5(e). Figures 5(c) and 5(d), recorded with circularly polarized light, do not show isogyres, but clearly reveal melatopes—the dark spots—which correspond to the optical axes. Figure 5(c) shows only one melatope in the centre. The two melatopes visible in Fig. 5(d) represent the two optical axes of the biaxial medium. Their lateral separation can be used to estimate the acute angle $2V_z$ between the axes. In our configuration of the conoscopic microscope, the image is a simple orthographic projection. Therefore, assuming that the total field of view corresponds to NA = 0.65, we find the angle V_z as $r/R = \sin(V_z)/\mathrm{NA}$, where $2r$ is a distance between the dark spots, and R is the radius of the field of view. This estimation gives $2V_z \approx 15°$, which, taking into account the error of our estimation method and the fact that the modified material is sandwiched between layers of pristine uniaxial material, is in very good agreement with the calculated value $2V_z = 19.14°$ (0.334 rad) at 633 nm (22.12° (0.386 rad) at 455 nm).

In conclusion, we have shown that combining form birefringence resulting from light-induced self-organized nanogratings with natural birefringence of MgO:$LiNbO_3$ transforms the crystal into an artificial biaxial medium—a 3D photonic nonlinear metamaterial. Because the material can be easily modified using a standard femtosecond laser-writing technique, various architectures with a characteristic size ranging from one to hundreds of micrometers can be easily obtained. The form birefringence and the acute angle between the optical axes of the resultant biaxial metamaterial can be controlled by adjusting the writing laser polarization, wavelength, pulse durations, repetition rates, etc. of the fundamental or second harmonic of the beam.

The engineered biaxial structures might be used for wavefront conversion similar to the nanogratings in glass. Glass-based elements can only exhibit simple birefringence, whereas biaxial structures can be employed for the formation of nontrivial vector beams not achievable otherwise. Furthermore, the nonlinearity of the host may provide an additional degree of freedom for final polarization and wavefront control of the second harmonic light generated in the structure.

This opens up new possibilities of creating structures suitable for low power, as in integrated optical devices, as well as those capable of handling high laser powers. The ability to form macroscopic volumes of a 3D dielectric photonic metamaterial with nonlinear optical properties is unique and not possible using metal or high-index dielectric metasurfaces. The self-organized nanogratings in lithium niobate have a great potential to become key components of low-loss artificial photonic crystals and metamaterials possessing strong nonlinear optical properties.

ACKNOWLEDGMENTS

The authors acknowledge the financial support from the Australian Research Council. W.K. acknowledges support from the Qatar National Research Fund (No. NPRP12S-0205-190047). P.K. thanks the Polish Ministry of Science and Higher Education for the "Mobility Plus" scholarship.

REFERENCES

[1]E. N. Glezer, M. Milosavljevic, L. Huang, R. J. Finlay, T.-H. Her, J. P. Callan, and E. Mazur, Opt. Lett. **21**, 2023 (1997).

[2]K. M. Davis, K. Miura, N. Sugimoto, and K. Hirao, Opt. Lett. **21**, 1729 (1996).
[3]S. J. Mihailov, C. W. Smelser, P. Lu, R. B. Walker, D. Grobnic, H. Ding, and J. Unruh, Opt. Lett. **28**, 995 (2003).
[4]A. Martinez, M. Dubov, I. Khrushchev, and I. Bennion, Electron. Lett. **40**, 1170 (2004).
[5]M. Beresna, M. Gecevičius, P. G. Kazansky, and T. Gertus, Appl. Phys. Lett. **98**, 201101 (2011).
[6]R. R. Gattass and E. Mazur, Nat. Photonics **2**, 219 (2008).
[7]R. Taylor, C. Hnatovsky, and E. Simova, Laser Photonics Rev. **2**, 26 (2008).
[8]D. Choudhury, J. R. Macdonald, and A. K. Kar, Laser Photonics Rev. **8**, 827 (2014).
[9]F. Chen and J. R. V. de Aldana, Laser Photonics Rev. **8**, 251 (2014).
[10]J. Burghoff, H. Hartung, S. Nolte, and A. Tünnermann, Appl. Phys. A Mater. Sci. Process. **86**, 165 (2007).
[11]C. Hnatovsky, R. S. Taylor, P. P. Rajeev, E. Simova, V. R. Bhardwaj, D. M. Rayner, and P. B. Corkum, Appl. Phys. Lett. **87**, 014104 (2005).
[12]C. B. Schaffer, A. Brodeur, and E. Mazur, Meas. Sci. Technol. **12**, 1784 (2001).
[13]M. Lancry, F. Zimmerman, R. Desmarchelier, J. Tian, F. Brisset, S. Nolte, and B. Poumellec, Appl. Phys. B Lasers Opt. **122**, 66 (2016).
[14]S. S. Fedotov, R. Drevinskas, S. V. Lotarev, A. S. Lipatiev, M. Beresna, A. Čerkauskaitė, V. N. Sigaev, and P. G. Kazansky, Appl. Phys. Lett. **108**, 071905 (2016).
[15]S. M. Eaton, H. Zhang, P. R. Herman, F. Yoshino, L. Shah, J. Bovatsek, and A. Y. Arai, Opt. Express **13**, 4708 (2005).
[16]C. B. Schaffer, J. F. García, and E. Mazur, Appl. Phys. A Mater. Sci. Process. **76**, 351 (2003).
[17]L. V. Keldysh, Sov. Phys. JETP **20**, 1307 (1965).
[18]V. P. Delone and N. B. Krainov, *Atoms in Strong Light Fields* (Springer-Verlag Berlin Heidelberg, 1985).
[19]Y. Shimotsuma, P. G. Kazansky, J. Qiu, and K. Hirao, Phys. Rev. Lett. **91**, 247405 (2003).
[20]V. R. Bhardwaj, E. Simova, P. P. Rajeev, C. Hnatovsky, R. S. Taylor, D. M. Rayner, and P. B. Corkum, Phys. Rev. Lett. **96**, 057404 (2006).
[21]C. Hnatovsky, D. Grobnic, D. Coulas, M. Barnes, and S. J. Mihailov, Opt. Lett. **42**, 399 (2017).
[22]S. Richter, C. Miese, S. Döring, F. Zimmermann, M. J. Withford, A. Tünnermann, and S. Nolte, Opt. Mater. Express **3**, 1161 (2013).
[23]F. Zhang, H. Zhang, G. Dong, and J. Qiu, J. Opt. Soc. Am. B **31**, 860 (2014).
[24]Y. Shimotsuma, T. Asai, M. Sakakura, and K. Miura, J. Laser Micro Nanoeng. **9**, 31 (2014).
[25]F. Zimmermann, M. Lancry, A. Plech, S. Richter, B. Hari Babu, B. Poumellec, A. Tünnermann, and S. Nolte, Opt. Lett. **41**, 1161 (2016).
[26]P. Karpinski, V. Shvedov, W. Krolikowski, and C. Hnatovsky, Opt. Express **24**, 7456 (2016).
[27]C. Hnatovsky, V. G. Shvedov, and W. Krolikowski, Opt. Express **21**, 12651 (2013).
[28]D. Wortmann, J. Gottmann, N. Brandt, and H. Horn-Solle, Opt. Express **16**, 1517 (2008).
[29]S. M. Rytov, Sov. Phys. JETP **2**, 466 (1956).
[30]A. Yariv and P. Yeh, *Optical Waves in Crystals* (John Wiley & Sons,Inc., New York, 1984).
[31]M. Born and E. Wolf, *Principles of Optics: Electromagnetic Theory of Propagation, Interference* (Cambridge University Press, 1999).
[32]E. Bricchi, B. G. Klappauf, and P. G. Kazansky, Opt. Lett. **29**, 119 (2004).
[33]T. Xu, K. Switkowski, X. Chen, S. Liu, K. Koynov, H. Yu, H. Zhang, J. Wang, Y. Sheng, and W. Krolikowski, Nat. Photonics **12**, 591 (2018).
[34]D. Wei, C. Wang, H. Wang, X. Hu, D. Wei, X. Fang, Y. Zhang, D. Wu, Y. Hu, J. Li, S. Zhu, and M. Xiao, Nat. Photonics **12**, 596 (2018).
[35]J. Thomas, V. Hilbert, R. Geiss, T. Pertsch, A. Tünnermann, and S. Nolte, Laser Photonics Rev. **7**, L17 (2013).
[36]S. Kroesen, K. Tekce, J. Imbrock, and C. Denz, Appl. Phys. Lett. **107**, 101109 (2015).
[37]J. Imbrock, H. Hanafi, M. Ayoub, and C. Denz, Appl. Phys. Lett. **113**, 252901 (2018).
[38]M. Triplett, J. Khaydarov, X. Xu, A. Marandi, G. Imeshev, J. Arntsen, A. Ninan, G. Miller, and C. Langrock, Opt. Express **27**, 21102 (2019).
[39]P. Török, P. Varga, and G. R. Booker, J. Opt. Soc. Am. A **12**, 325 (1995).
[40]C. Hnatovsky, R. S. Taylor, E. Simova, V. R. Bhardwaj, D. M. Rayner, and P. B. Corkum, J. Appl. Phys. **98**, 013517 (2005).
[41]Y. Shimotsuma, K. Hirao, J. Qiu, and P. G. Kazansky, Mod. Phys. Lett. B **19**, 225 (2005).
[42]J. A. Fleck, Jr. and M. D. Feit, J. Opt. Soc. Am. **73**, 920 (1983).
[43]A. Ciattoni, B. Crosignani, and P. Di Porto, J. Opt. Soc. Am. A. Opt. Image Sci. Vis. **18**, 1656 (2001).
[44]G. Zhou, A. Jesacher, M. J. Booth, T. Wilson, A. Ródenas, D. Jaque, and M. Gu, Opt. Express **17**, 17970 (2009).
[45]D. E. Zelmon, D. L. Small, and D. Jundt, J. Opt. Soc. Am. B **14**, 3319 (2008).
[46]R. S. Weis and T. K. Gaylord, Appl. Phys. A Solids Surfaces **37**, 191 (1985).
[47]C. Hnatovsky, E. Simova, P. P. Rajeev, D. M. Rayner, P. B. Corkum, and R. S. Taylor, Opt. Lett. **32**, 1459 (2007).
[48]J. Olivares, G. García, A. García-Navarro, F. Agulló-López, O. Caballero, and A. García-Cabañes, Appl. Phys. Lett. **86**, 183501 (2005).
[49]A. Emoto, M. Nishi, M. Okada, S. Manabe, S. Matsui, N. Kawatsuki, and H. Ono, Appl. Opt. **49**, 4355 (2010).
[50]V. G. Dmitriev, G. G. Gurzadyan, and D. N. Nikogosyan, *Handbook of Nonlinear Optical Crystals* (Springer, Berlin, 1999).
[51]J. R. Mourant, J. P. Freyer, A. H. Hielscher, A. A. Eick, D. Shen, and T. M. Johnson, Appl. Opt. **37**, 3586 (1998).
[52]C. F. Bohren and D. R. Huffman, *Absorption and Scattering of Light by Small Particles* (Wiley, 1998).
[53]Y. Pochi and G. Claire, *Optics of Liquid Crystal Displays* (John Wiley & Sons, 1999).
[54]N. H. Hartshorne and A. Stuart, *Crystals and the Polarizing Microscope* (Arnold, London, 1970).
[55]P. Wang, Opt. Lett. **37**, 4392 (2012).